The comparison of different temporal phase analysis algorithms in optical dynamic measurement

Miao, Hong; Fu, Yu

2008

Miao, H., & Fu, Y. (2008). The comparison of different temporal phase analysis algorithms in optical dynamic measurement. Ninth International Symposium on Laser Metrology, 7155, pp.1-10.

https://hdl.handle.net/10356/91915

https://doi.org/10.1117/12.814544

The comparison of different temporal phase analysis algorithms in optical dynamic measurement

H. Miao[a], Y. Fu[*,b]
[a]Dept. of Modern Mechanics, University of Science and Technology of China, Hefei, 230027.China
[b]Dept. of Mechanical Engineering, National University of Singapore, 10 Kent Ridge Crescent, Singapore 119260

ABSTRACT

In recent years, optical interferometry has been applied to whole-field, non-contact measurement of vibrating or continuously-deforming objects. In optical dynamic measurement, an interferogram sequence is obtained by a high-speed camera. Retrieving dynamic phase values from this interferogram sequence leads to a precise measurement of different kinematic and deformation parameters of a continuously-deforming or vibrating object. In this paper, this interferogram sequence is classified into two types: (i) intensity variation; and (ii) exponential phase signal. Different temporal phase retrieving techniques, such as Hilbert transform, Fourier transform, windowed Fourier transform and wavelet transform are applied to extract the phase from a simulated signal. The advantage and drawback of each algorithm are discussed. In addition, a new method based on the combination of Fourier transform and windowed Fourier transform is proposed and the simulation shows it can eliminate the noise and evaluate the phase more accurately.

Keywords: Temporal phase extraction, vibration measurement, wavelet transform, Fourier analysis, digital holography.

1. INTRODUCTION

Optical interferometric techniques such as geometric moiré, holography, moiré interferometry and shearography have been developed for the measurement of a wide range of physical parameters, such as displacement, strain, surface profile, and refractive index. Since the 1960's, optical interferometry has been applied to whole-field, non-contact dynamic measurement. For high-frequency vibration, optical interferometry is normally applied to the determination of vibration modes of objects by the time-average methods[1]. However, the time-average method is not suitable to measure the transient deformation of a continuously-deforming object or a vibrating object. The use of a twin-cavity double-pulsed laser in the interferometry[2,3] has been reported as an alternative to obtain these transient deformations. Unfortunately, this technique has an important limitation. To obtain the evolution of the transient deformation, an experiment must be repeated many times with a different interval of two pulses. This means non-repeatable events cannot be studied in detail.

With the availability of high-speed digital recording and powerful laser, it is now possible to record interferograms with rates exceeding 100,000 frames per second (fps). Sometimes these interferograms are pre-processed to a sequence of wrapped 2-D phase maps by different techniques, such as a carrier-based 2-D Fourier analysis[4] or a reconstruction of a digital hologram sequence[5]. Normally these wrapped phase maps are noisy and are not suitable for spatial phase unwrapping. In the 1990's, a new phase evaluation method based on temporal analysis[6,7] was introduced. It analyzes the phase point by point along the time axis, so that the speckle noise in adjacent pixels does not affect the measurement. In addition, it expands the displacement measurement range to more than 500μm[8]. A Fourier transform[9] is usually applied to extract the phase in the temporal domain. In recent years, Hilbert transform[10], windowed Fourier transform(WFT)[11,12] and continuous wavelet transform(CWT)[13-15] have also been introduced for temporal phase extraction. In addition, WFT and CWT can also extract the instantaneous frequency of the temporal intensity variation from which the velocity of the deformation can be evaluated.

The temporal phase analysis technique has its own disadvantage: when the intensity variations of pixels are analyzed, it cannot extract the phase from a part of an object that is not moving with the rest or from objects that deform in different directions at different parts. Without a temporal carrier[9,15], neither Fourier analysis nor wavelet analysis

Ninth International Symposium on Laser Metrology, edited by Chenggen Quan, Anand Asundi
Proc. of SPIE Vol. 7155, 715518, (2008) · 0277-786X/08/$18 · doi: 10.1117/12.814544

allows the determination of the absolute sign of the phase. This limits the technique to the measurement of deformation in one known direction. Similar to a spatial carrier, a temporal carrier can also be introduced in the image acquisition process to overcome these problems, at the cost of a reduced measurement range of phase variation.

In this paper, the temporal signals on each pixel are classified into two types: (I) Intensity variation with a known uniform direction of phase change; and (II) exponential phase signal. These two types of signal will be processed by those four algorithms mentioned above. The advantages and disadvantages of each algorithm will be presented based on the processing of simulated signals. A new method based on the combination of Fourier transform and windowed Fourier transform will be proposed for the temporal analysis of intensity variation signal, in order to eliminate the noise effect and to evaluate the kinematic parameters more accurately.

2. SIGNALS AND PROCESSING ALGORITHMS

In high-speed optical dynamic measurement, a sequence of interferograms is captured by a high-speed camera. These interferograms could be a sequence of original speckle or fringe patterns or a sequence of wrapped phase map after pre-processing. The pre-processing could be a reconstruction of a digital hologram, a high-speed phase-stepping processing or a carrier-based Fourier analysis. Processing of these 3-D intensity or wrapped phase matrices enable the measurement of kinematic and deformation parameters of the object. A one-dimensional temporal process on each pixel is usually the first step of the analysis.

2.1 Two types of Signal

In this paper, the temporal signals on each pixel are classified into two types: (I) Intensity variation with a known uniform direction of phase change; and (II) exponential phase signal. The first type of signal on point *P(x, y)* can be written as:

$$f_I(x,y;t) = I_b(x,y;t) + A(x,y;t)\cos\left(\varphi(x,y;t)\right) \tag{1}$$

where $I_b(x,y;t)$ and $A(x,y;t)$ are the intensity bias and the modulation factor, respectively. These two items are both slowly varying functions along time axis. $\varphi(x,y;t) = \varphi_C(t) + \varphi_O(x,y;t)$ is a single-directional phase variation of the signal of each pixel. In ESPI, it can be obtained for a continuously-deforming object, where all points are deforming in a known direction or on a vibrating object with a temporal carrier. $\varphi_C(t)$ is the phase change due to the temporal carrier; it is normally uniform for each pixel. $\varphi_O(x,y;t)$ is the phase variation due to a vibration or displacement with an unknown direction. The temporal carrier frequency should be high enough that the phase change at each pixel is only in one direction. In addition, the signal frequency component should be separable from the zero-frequency components, but able to be sampled according to the Nyquist theorem. In general, the introduction of a temporal carrier will reduce the measurement range of deformation velocity.

The second type of temporal signal is the exponential phase signal:

$$f_{II}(x,y;t) = \exp\left(j\cdot\phi(x,y;t)\right), \tag{2}$$

where $j=\sqrt{-1}$ and $\phi(x,y;t)$ is the phase value on point *P(x, y)* at instant *t*. It is worth noting that the phase ambiguity problem mentioned above does not exist in the exponential phase signal. The phase variation could be in both directions. No temporal carrier is needed. However, a carrier is still necessary for obtaining the phase signal itself, either by standard FT or dynamic phase shifting[16]. This carrier also exists in digital holography, arising from the small angle between object and reference beams. In this investigation, these two types of signal are processed by following different signal processing techniques.

2.2 Processing algorithms

(1) Fourier transform

The Fourier analysis is the most popular method in temporal phase extraction. The Fourier transform of a one-dimensional temporal signal $f(t)$ can be expressed as:

$$\hat{f}(\xi) = \int_{-\infty}^{+\infty} f(t)\exp(-j\xi t)dt \tag{3}$$

where $\hat{f}(\xi)$ is the Fourier transform of $f(t)$. Normally the Fourier spectrum is filtered by a bandpass filter and the inverse Fourier transform yields an exponential signal $C(t)$ from which the phase can be calculated by:

$$\varphi(t) = \arctan\frac{\mathrm{Im}(C(t))}{\mathrm{Re}(C(t))} \tag{4}$$

where Im and Re denote the imaginary and real parts of $C(t)$, respectively. The phase obtained is wrapped between $-\pi$ to $+\pi$. A 1-D temporal unwrapping procedure is needed to reconstruct the continuous phase function $\varphi(t)$. A similar process can be applied when $f(t)$ is an exponential signal, as shown in Eq. (2). The spectrum of an exponential signal could be in both positive and negative frequency areas, but with the DC terms and the conjugate terms absent. It is well known that the accuracy of a Fourier transform analysis increases with the decrease of the width of the spectrum. However, when the phase change of the signal is highly nonlinear, the width of the side band in the spectrum increases. This occurs quite often in dynamic measurements as the velocity of the object is normally varying. In addition, different pixels have different spectra. The selection of a proper window for bandpass filtering for all pixels becomes difficult.

(2) Hilbert transform

Hilbert transform(HT) can only be used to process real signal, in our case, the intensity variation signal f_I. The HT of f_I is defined by

$$Hi(f(t)) = \frac{1}{\pi}\int_{-\infty}^{+\infty}\frac{f(t')}{t'-t}dt' = -\frac{1}{\pi t}\otimes f(t) \tag{5}$$

where $\otimes$ denotes the convolution. The HT of the signal $\cos(\varphi(t))$ gives $\sin(\varphi(t))$. The phase of the signal can be determined by

$$\varphi(t) = \arctan\left(\frac{Hi(f(t))}{f(t)}\right) \tag{6}$$

It is worth noting that the bias intensity $I_b(t)$ in Eq. (1) has to be removed before the Hilbert transform. It is equivalent to Fourier analysis with a bandpass filter width of (0, π). Therefore it extracts the phase without any noise elimination effects.

(3) Windowed Fourier transform

A one-dimensional windowed Fourier transform (WFT) of a temporal signal $f(t)$ and can be written as[17]:

$$Sf(u,\xi) = \int_{-\infty}^{+\infty} f(t)g^*_{u,\xi}(t)dt \tag{7}$$

where $Sf(u,\xi)$ denotes the spectrum of WFT; and $g_{u,\xi}(t)$ is the WFT kernel, which can be expressed as $g_{u,\xi}(t) = g(t-u)\exp(j\xi t)$. The window $g(t)$ is usually chosen as the Gaussian function: $g(t) = \exp(-t^2/2\sigma^2)$ which permits the best time-frequency localization in analysis. σ is a parameter to control the expansion of the window size. Figure 1(a) shows the real part of a windowed Fourier kernel at different frequencies: 0.1π, 0.2π, and 0.3π when $\sigma = 20$. Their spectrums are shown in Fig. 1(b). It can be observed that the window size remains the same at different frequencies. The instantaneous frequency of signal $\xi(u) = \varphi'(u)$ can be obtained by extracting the 'ridge' on the spectrum of WFT[17]. A filtered signal phase can be obtained by integration. For an intensity varying signal f_I, the direct use of a WFT may generate a large error, due to the effect of the DC term and even the negative frequency. This problem will be illustrated with a simulated signal in the next section.

A windowed Fourier transform maps a 1-D temporal signal to a 2-D time-frequency plane, and extracts the signal's instantaneous frequency. Thus it is more effective to remove the noise within the frequency band of the signal. This is the advantage of WFT over Fourier transform. However, the time-frequency uncertainty principle affects the resolution, which leads to trade-off between time and frequency localization. Once the window size is determined, WFT has a uniform resolution at different frequencies. In many cases, a high frequency resolution is needed when the signal frequency is low, and a low frequency resolution can be accepted when signal frequency is high. This leads to another signal processing algorithm, the wavelet transform.

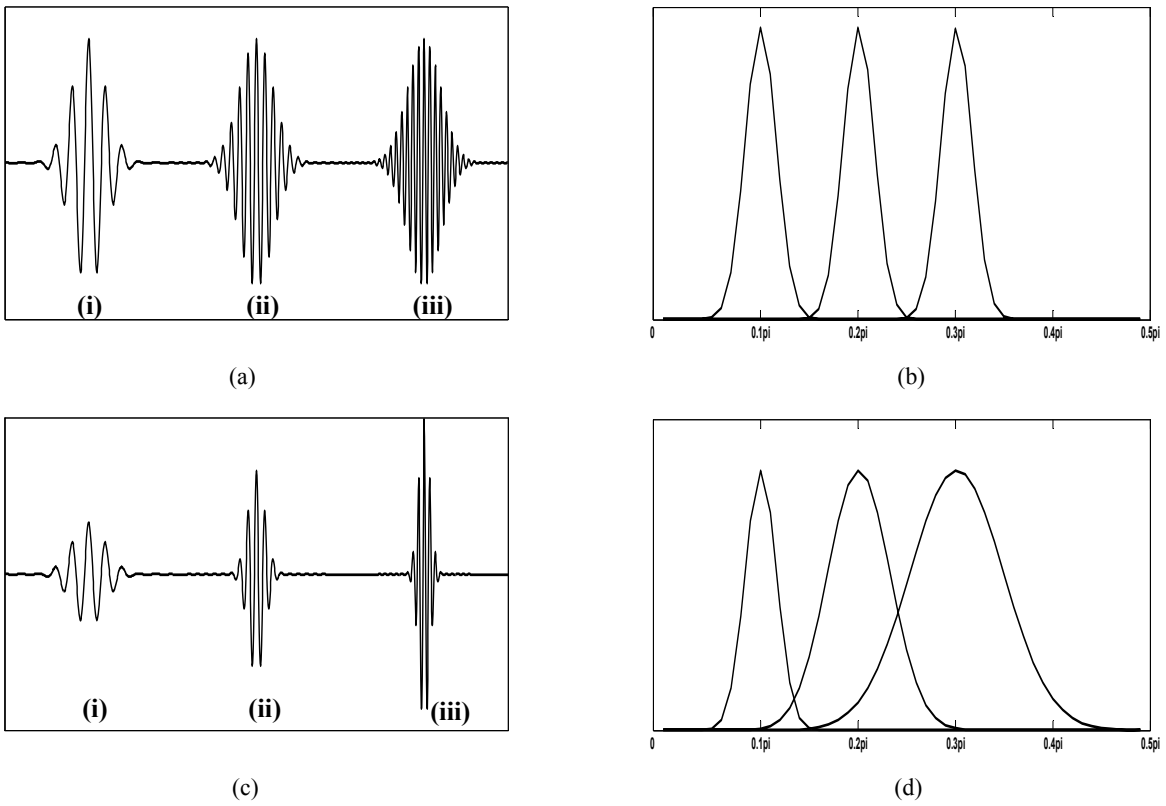

Fig. 1 (a) real part of a windowed Fourier kernel at different frequencies: 0.1π, 0.2π, and 0.3π; the window size is set as $\sigma = 20$; (b) the spectrum of windowed Fourier kernels in (a); (c) real part of a complex Morlet wavelet at different frequencies: $0.1\pi, 0.2\pi$, and 0.3π (a=20, 10 and 6.67); (d) the spectrum of complex Morlet wavelets in (c).

(4) Wavelet transform

Wavelet transform (WT) is similar to windowed Fourier transform, but with a varying window size according to the signal frequency. A wavelet transform of an intensity varying signal f_I can be expressed as:

$$Wf(a,b) = \frac{1}{\sqrt{a}} \int_{-\infty}^{+\infty} f(t) \Psi^* \left(\frac{t-b}{a} \right) dt = \frac{1}{\sqrt{a}} \int_{-\infty}^{+\infty} f(t) \Psi_{ab}^*(t) dt \tag{8}$$

where $\Psi(t)$ is known as the mother wavelet, and $\Psi_{ab}(t)$ are the basis functions of the transform, known as daughter wavelets. *a* is the scaling factor related to the frequency and *b* is the time shift. While similar to the WFT mentioned above, it is more appropriate to use a complex function as the mother wavelet, in order to properly separate the phase and amplitude information of the signal. The most commonly-used mother wavelet for such an application is the complex Morlet wavelet, which is the product of a real Gaussian window and a complex oscillating exponential function:

$$\Psi(t) = g(t) \exp(i\omega_0 t) \tag{9}$$

where $g(t) = \exp\left(-t^2/2\right)$. ω_0 is the "mother" frequency or central frequency, this is the only parameter that has to be selected. The different wavelets used during time-frequency analysis are derived from the mother wavelet by a scaling *a* and time shift *b*. In order to satisfy the admissibility condition, ω_0 must be large than five. A proper selection of the central frequency ω_0 determines the overall "balance" between time and frequency resolution. In this study, ω_0 is selected as 2π to satisfy the admissibility condition and to keep the flexibility of the wavelet analysis. Figure 1(c) shows the real part of a complex Morlet wavelet at different frequencies: $0.1\pi, 0.2\pi$, and 0.3π (a=20, 10 and 6.67). Their spectrums are shown in Fig. 1(d). It can be observed that the extent of the analysis window in the wavelet transform varies according to the analysis frequency ξ.

As for the WFT, the instantaneous frequency of the signal can also be extracted from the wavelet ridge:

$$\varphi'(b) = \xi_{rb} = \frac{\omega_0}{a_{rb}} \tag{10}$$

where a_{rb} denotes the value of a at the instant b on the ridge.

3. SIMULATION AND DISCUSSION

3.1 Simulation on intensity variation signal

Figure 2(a) shows a simulated temporal intensity variation of a vibrating object with a temporal carrier. Some random noise is added to the signal. The noise is set as 5% of the signal amplitude. Figure 2(b) and 2(c) show the theoretical phase value $\varphi(t)$ and its first-order derivative $\varphi'(t)$. Figure 2(d) is the Fourier spectrum of the signal. The dotted line roughly indicates the signal frequency band which is quite broad.

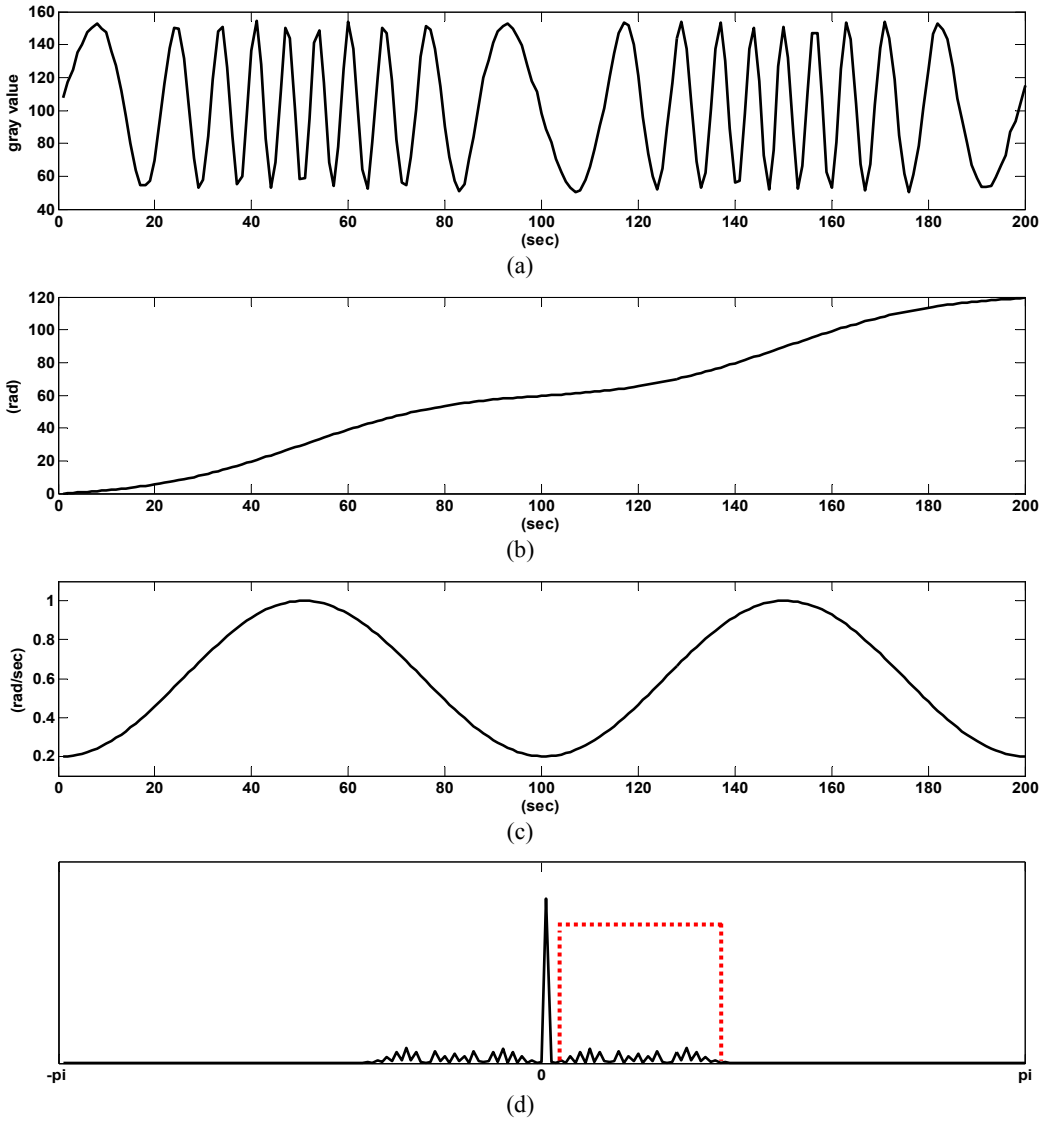

Fig. 2 (a) a simulated intensity variation on a vibrating object with a temporal carrier; (b) the theoretical phase value of signal in (a); (c) the first-order derivative of the phase value; (d) the Fourier spectrum of the signal;

In the processing of a real signal where the position frequency, DC term and negative frequency are separable, it is worth noting that:

[1] A Fourier transform always gives a reasonable result when a proper filtering window is selected. However, FT cannot remove the noise whose frequency is superimposed on the signal frequency; therefore, the accuracy is not very high when the signal frequency band is broad.

[2] Hilbert transform performs the worst in noise elimination as the equivalent bandpass filtering window is $(0, \pi)$.

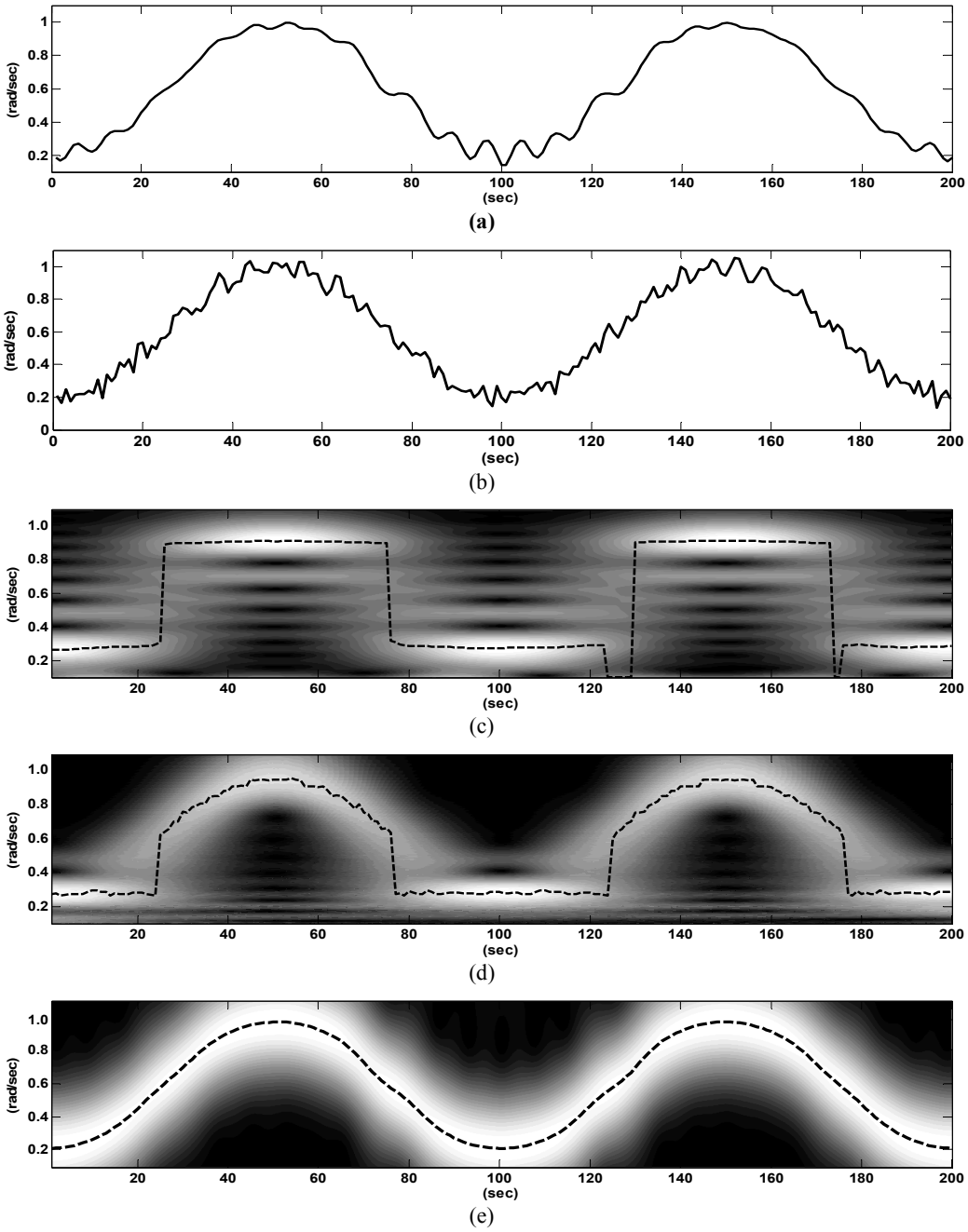

Fig. 3 the first-order derivative of the phase obtained by (a) Fourier bandpass filtering and (b) Hilbert transform and a numerical differentiation; (c) modulus of the windowed Fourier transform when $\sigma = 20$ and the corresponding ridge; (d) modulus of the wavelet transform and the corresponding ridge; (e) the ridge obtained by combination of FFT and WT processing.

[3] In WFT, the window size σ_t is determined by several factors: (a) In WFT, the signal phase is assumed to be linear in the area covered by the Gaussian window. However, in temporal analysis it is normal that the frequency varies dramatically. Hence the window size should be small in order to reduce the linear phase approximation error; (b) a larger window size performs better in noise elimination. However, in temporal analysis, the signal is not very noisy even in speckle interferometry as the intensity variation is analyzed pixel by pixel. Normally selecting a large window size is not necessary; (c) a windowed Fourier kernel with a small window size in time will have large window size in the spectrum. When the low frequency part of the signal is processed, the result will be seriously affected by the DC term. Accordingly to our experience, for a certain signal frequency ξ, the window size in time should satisfy $\sigma_t \geq 2.0/\xi$ to avoid the influence of the DC term; (d) A compromise between (a) and (b) is not difficult in temporal analysis. However, the conflict between (a) and (c) is inevitable in many cases and will usually cause large system error. One of the solutions is to remove the DC term before the WFT.

[4] In the wavelet transform, the influence of the DC term can be ignored when $\omega_0 > 5$. However, the wavelet transform performs very poorly when the signal frequency is low, as it will automatically adjust the window size σ_t to be very large, sometimes even larger than the signal length. This will generate large errors in the phase extraction. Normally a wavelet transform only performs well when the signal frequency is high and has small variation.

Figure 3(a) shows the first-order derivative of the phase obtained by a Fourier bandpass filtering and a numerical differentiation. The noise effect is still quite obvious in the FT result. Figure 3(b) shows the results from Hilbert transform. High frequency noise can be observed as no filtering process is involved. Figure 3(c) shows the modulus of the windowed Fourier transform. The dashed line shows the ridge where the maximum moduli are found. $\sigma = 20$ is selected as a window size to avoid the influence of the DC term. However, it is obviously not sensitive enough to the frequency variation. This is due to the conflict of points (a) and (c) in the WFT process mentioned above. Figure 3(d) shows the wavelet ridge of the signal. The wavelet transform performs well in a high frequency range, but gives incorrect results in the low frequency range. The main problem involved is that the window size σ_t selected automatically by wavelet transform is not small enough, so that the linear phase approximation error seriously affects the result.

So far Fourier transform performs the best in the first-order phase derivative extraction. A new processing technique based on the combination of Fourier transform and windowed Fourier transform is suggested here to improve the result. An intensity varying signal is processed by FT and bandpass filtering so that the negative frequency and DC term are removed. The wrapped phase obtained by FT is converted to an exponential phase signal f_{II} and then processed again by a WFT with a small σ_t. Figure 3(e) shows the results from a FT+WFT processing. $\sigma_t = 4$ is selected for the WFT window size. A perfect WFT ridge is obtained this time.

From the simulation results shown above, it can be concluded that for a real signal of temporal intensity variation f_I, it is better to convert it to an exponential phase signal f_{II} first by a Fourier analysis and then to process it by windowed Fourier transform.

3.2 Simulation on exponential phase signal

In the temporal analysis of an exponential phase signal f_{II}, a temporal carrier is not necessary as the phase ambiguity problem does not exist. For a vibrating object, the spectrum of this exponential signal f_{II} will contain values around the zero frequency, with a certain bandwidth from negative to positive frequencies. The width of the spectrum depends on the value of the second-order derivative of the phase, in this case the acceleration. The purpose of the processing is the filtering of the noise and the extraction of the derivatives of the phase, which lead to the measurement of some other useful physical properties. In a windowed Fourier analysis, the conflict of conditions (a) and (c) mentioned above does not exist. Therefore applying a FT analysis before the WFT is not necessary. Hilbert transform is only suitable to process the real signal. Due to the poor performance of the wavelet transform at low-frequency, it is not practical to process the signal when the frequency is around zero. In this case, we only compare the FT and WFT on extraction of the phase and its derivatives.

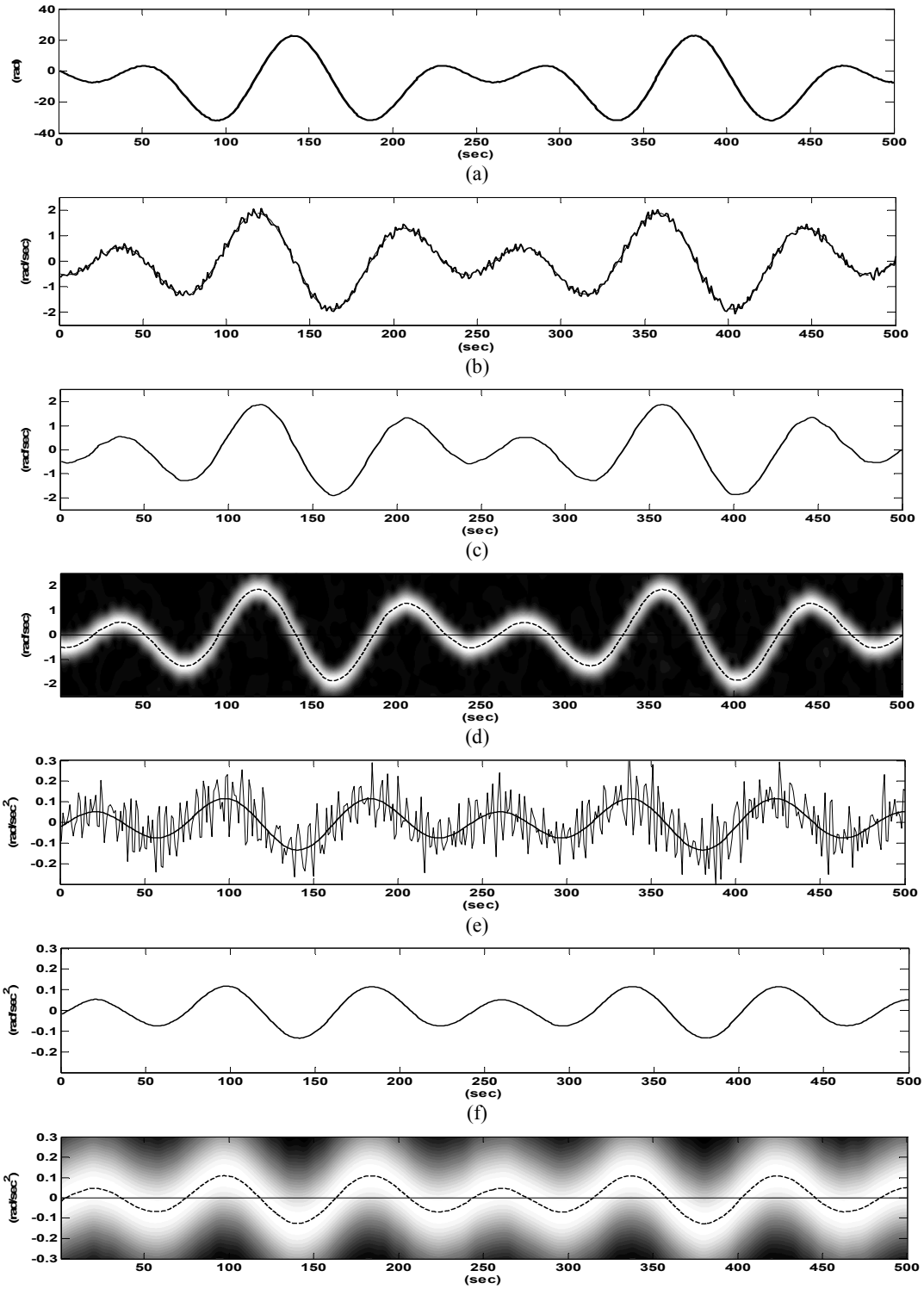

Fig. 5(a) A simulated phase variation with noise containing two vibration frequencies; (b) The first derivative of (a) with and without noise; (c) The first derivative of (a) after low-pass filtering; (d) The first derivative of (a) obtained by windowed Fourier ridge;(e) The second derivative of (a) with and without noise; (f) The second derivative of (a) after low-pass filtering; (g) The second derivative of (a) obtained by windowed Fourier ridge.

Figure 5(a) shows a simulated phase variation with some additive random noise. The signal includes two frequencies, 80 point/frame and 120 point/frame. Suppose the time interval between two adjacent frames is 1 sec, the maximum velocity measurement range of this method is within $(-\pi, \pi)$ rad/sec, due to the constraint of the Nyquist sampling theorem. Figure 5(b) shows the numerical differentiation of the signal and the smooth line which is the first derivative of the ideal value without noise. The simulated phase variation is converted to exponential phase signal. The result of the first derivative from above-mentioned Fourier analysis is shown in Fig. 5(c). The relative error is more than 10%. Figure 5(d) shows the modulus of the windowed Fourier transform of the simulated signal [Fig. 5(a)]. The dashed line shows the ridge of where the maximum moduli are found. The $\sigma = 4$ is selected as window size. An accurate velocity is obtained with the relative error less than 2%.

A similar process is repeated to obtain the second derivative. Figure 5(e) shows the second derivative of signal with and without noise. This time the spectrum of the exponential signal is much narrower and a relatively small filtering window size can be selected. Figure 5(f) is the second derivative of the phase variation obtained by Fourier analysis. The relative error is only 3%. In WFT the window size is selected as $\sigma = 8$. Figure 5(g) shows the windowed Fourier ridge. Although it is also a very smooth signal, a slight offset in frequency can be observed and a relative error of 7% is found compared with the ideal second derivative.

From the above simulation on exponential phase signal, it can be observed that in the first derivative evaluation, as the spectrum of the signal is broad, the windowed Fourier ridge method shows its capability in instantaneous frequency extraction and noise reduction, thus performs better than Fourier analysis. However in the second derivative evaluation, the spectrum of signal is narrow, Fourier analysis also performs well in eliminating the noise. Thus it is recommended due to its fast processing speed.

4. CONCLUSTION

In this paper we have presented different processing algorithms for temporal phase analysis of two simulated temporal signals. For an intensity varying signal, a Fourier analysis is necessary to remove the influence of the DC term and to convert the real signal to an exponential phase signal. However, a Fourier analysis cannot remove noise whose frequencies are superimposed with signal frequencies. Windowed Fourier analysis then becomes a typical processing technique to filter the noise and to extract the derivatives of the phase. Instantaneous kinematic parameters, such as displacement, velocity and acceleration, can be obtained by temporal analysis. The criteria for the selection of window size in WFT were also discussed. A large window size performs better in noise elimination, but generates more error when the signal phase variation is nonlinear. The processing results on simulation and experiment show the capability of WFT in phase and phase derivatives extraction. Compared to WFT, the application of wavelet transform is limited due to the poor performance in the low-frequency part. Similar situations are found in 2D spatial and 3D spatio-temporal analysis for deformation parameters evaluation when the Nyquist sampling theorem is satisfied along all axes. The proposed algorithms show that it is now possible to have a whole-field, non-contact optical measurement of different useful parameters.

ACKNOWLEDGEMENTS

The authors gratefully acknowledge the financial support provided by the National Science Foundation of China (NSFC) under contract number 10772171 and 10732080.

REFERENCES

1. Nakadate S., "Vibration measurement using phase-shifting time-average holographic interferometry," *Appl. Opt.* **25,** 4155-4161 (1986).
2. Schedin S., Pedrini G., Tiziani H. J. and Santoyo F. M., "Simultaneous three-dimensional dynamic deformation measurements with pulsed digital holography," *Appl. Opt.* **38,** 7056-7062 (1999).
3. Pedrini G., Tiziani H. and Zou Y., "Digital double pulse-TV-holography," *Opt. Laser Eng.* **26**, 199-219 (1997).

4. Takeda M., Ina H. and Kobayashi S., "Fourier-transform method of fringe-pattern analysis for computer-based topography and interferometry," *J. Opt. Soc. Am.* **72**, 156-160 (1982).
5. Pedrini G., Osten W. and Gusev M. E., "High-speed digital holographic interferometry for vibration measurement," *Appl. Opt.* **45**, 3456-3462 (2006).
6. Huntley J. M. and Saldner H., "Temporal phase-unwrapping algorithm for automated interferogram analysis," *Appl. Opt.* **32**, 3047-3052 (1993).
7. Joenathan C., Franze B., Haible P. and Tiziani H. J., "Speckle interferometry with temporal phase evaluation for measuring large-object deformation," *Appl. Opt.* **37**, 2608-2614(1998).
8. Tiziani H. J., "Spectral and temporal phase evaluation for interferometry and speckle applications," in *Trends in Optical Nondestructive Testing and Inspection*, P. K. Rastogi and D. Inaudi, eds. (Elsevier Science B. V. Amsterdam, 2000). pp323-343.
9. Kaufmann G. H., "Phase measurement in temporal speckle pattern interferometry using the Fouier transform method with and without a temporal carrier," *Opt. Commun.* **217**,141-149 (2003).
10. Madjarova V. D., Kadona H. and Toyooka S. "Dynamic electronic speckle pattern interferometry (DESPI) phase analyses with temporal Hilbert transform," *Opt. Express.* 11(6), 617-623 (2003).
11. Qian K., "Windowed Fourier transform for fringe pattern analysis," *Appl. Opt.* **43**, 2695-2702 (2004).
12. Fu Y., Pedrini G. and Osten W., "Vibration measurement by temporal Fourier analyses of digital hologram sequence", *Appl. Opt.* **46**, 5719-5727 (2007).
13. Colonna de Lega X., "Processing of non-stationary interference patterns: adapted phase shifting algorithms and wavelet analysis. Application to dynamic deformation measurements by holographic and speckle interferometry," Thesis 1666, Swiss Federal Institute of Technology, Lausanne, Switzerland, (1997).
14. Fu Y., Tay C. J., Quan C. and Chen L. J., "Temporal wavelet analysis for deformation and velocity measurement in speckle interferometry," *Opt. Eng.* **43**, 2780-2787 (2004).
15. Fu Y., Tay C. J., Quan C. and Miao H., "Wavelet analysis of speckle patterns with a temporal carrier," *Appl. Opt.* **44**, 959-965 (2005).
16. Colonna de Lega X. and Jacquot P., "Deformation measurement with object-induced dynamic phase shifting," Appl. Opt. **35**, 5115-5121 (1996).
17. Mallat S., *A wavelet Tour of Signal Processing,* (Academic Press, San Diego, Calif., 1998).